



**Enabling Multi-Electron Reaction of  $\epsilon$ -VOPO<sub>4</sub> to Reach Theoretical Capacity for Lithium-ion Batteries**

Journal:	<i>ChemComm</i>
Manuscript ID	CC-COM-03-2018-002386.R1
Article Type:	Communication

SCHOLARONE™  
Manuscripts

## Enabling Multi-Electron Reaction of $\epsilon$ -VOPO<sub>4</sub> to Reach Theoretical Capacity for Lithium-ion Batteries

Received 00th January 20xx,  
Accepted 00th January 20xx

DOI: 10.1039/x0xx00000x

www.rsc.org/

Carrie Siu,<sup>a</sup> Ieuan D. Seymour,<sup>b</sup> Sylvia Britto,<sup>b</sup> Hanlei Zhang,<sup>a</sup> Jatinkumar Rana,<sup>a</sup> Jun Feng,<sup>a</sup> Fredrick O. Omenya,<sup>a</sup> Hui Zhou,<sup>a</sup> Natasha A. Chernova,<sup>a</sup> Guangwen Zhou,<sup>a</sup> Clare P. Grey,<sup>b</sup> Louis F. J. Piper,<sup>a</sup> M. Stanley Whittingham<sup>a</sup>

**By controlling the morphology and particle size of the epsilon polymorph of vanadyl phosphate,  $\epsilon$ -VOPO<sub>4</sub>, it can fully reversibly intercalate two Li-ions and reach the theoretical capacity of 305 mAh/g over two voltage plateaus at about 4.0 and 2.5 V.**

One key way to increase the energy density of Li-ion batteries is to use cathode materials that are capable of reversibly intercalating more than 1 Li<sup>+</sup> per redox centre. Vanadium phosphate compounds are suitable candidates as they provide two redox transitions, V<sup>5+</sup>/V<sup>4+</sup> and V<sup>4+</sup>/V<sup>3+</sup>, within a stable electrolyte voltage window.<sup>1-7</sup> The  $\epsilon$ -VOPO<sub>4</sub>  $\leftrightarrow$   $\epsilon$ -LiVOPO<sub>4</sub>  $\leftrightarrow$   $\epsilon$ -Li<sub>2</sub>VOPO<sub>4</sub> system has been regarded as one of the most promising and safe candidates to provide a two-electron reaction with high theoretical capacity of 305 mAh/g coming from V<sup>5+</sup>/V<sup>4+</sup> reaction at 4.0 V and V<sup>4+</sup>/V<sup>3+</sup> at 2.5 V, resulting in specific energy over 900 Wh/g.<sup>8,13,16,17</sup>  $\epsilon$ -VOPO<sub>4</sub> was first synthesized by Lim et al. by heating monoclinic H<sub>2</sub>VOPO<sub>4</sub> in oxygen, and Kerr et. al measured the reversible electrochemistry at the high voltage plateau at 4.0 V.<sup>9,10</sup> Previously, we have reported the synthesis and characterization of  $\epsilon$ -VOPO<sub>4</sub> from two different phases of H<sub>2</sub>VOPO<sub>4</sub> to discover that the electrochemical performance from the disordered tetragonal precursor was improved due to smaller particle size.<sup>11</sup> We also conducted fundamental studies on the structural evolution of  $\epsilon$ -LiVOPO<sub>4</sub> and identified two intermediate phases in the low-voltage regime using DFT calculations backed up with X-ray pair distribution function analysis and X-ray absorption near edge structure measurements, first proposed by Bianchini et. al.<sup>12,13,17</sup> However, the latest electrochemistry of  $\epsilon$ -VOPO<sub>4</sub> reported is far from theoretical, with a large hysteresis between discharge and charge profiles. In this paper, the full electrochemical reversible insertion of two Li-ions into  $\epsilon$ -VOPO<sub>4</sub> is demonstrated for the first time, reaching the theoretical

specific capacity of 305 mAh/g. This is attributed to crystalline nano-particles of controlled morphology that originated from the hydrothermally synthesized H<sub>2</sub>VOPO<sub>4</sub> precursor. Hydrothermal synthesis has many unique advantages because it offers good control over the sample's purity and crystallinity, is easy to scale up, and low cost. This method can keep the overall particle size small and size distribution narrow which are vital features for good cathodic electrochemical performance.<sup>14</sup> We have observed that the morphology of the H<sub>2</sub>VOPO<sub>4</sub> precursor and the corresponding  $\epsilon$ -VOPO<sub>4</sub> product is affected by the hydrothermal solvent. By using 95% ethanol in H<sub>2</sub>VOPO<sub>4</sub> hydrothermal synthesis,  $\epsilon$ -VOPO<sub>4</sub> with loose particle morphology is obtained (Figure 1a), whereas 100% ethanol results in the agglomeration of primary particles, leading to the formation of secondary particles of 2  $\mu$ m balls. (See ESI Figure 1) Figure 1a shows the as-synthesized  $\epsilon$ -VOPO<sub>4</sub> powder composed of primary particles of ~100-200 nm that are cuboid in shape.

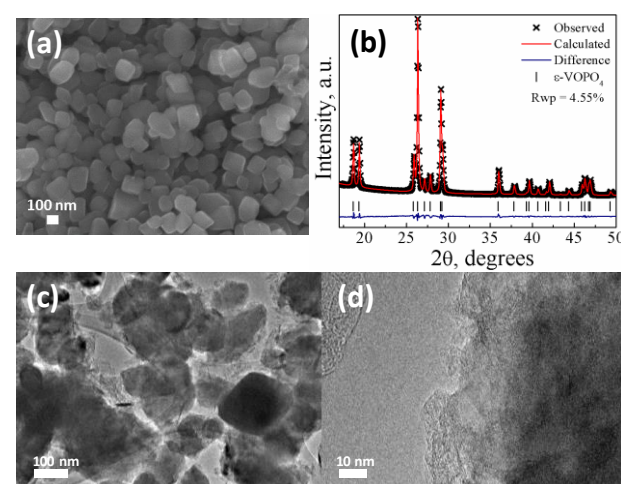


Figure 1. (a) SEM image and (b) XRD pattern with Rietveld refinement of the as synthesized  $\epsilon$ -VOPO<sub>4</sub> material. (c, d) TEM images of  $\epsilon$ -VOPO<sub>4</sub> particles hand mixed with graphene nanoplatelets for slurry preparation.

<sup>a</sup> NorthEast Center for Chemical Energy Storage (NECCES) at Binghamton University in Binghamton, NY, 13902, USA

<sup>b</sup> Department of Chemistry at University of Cambridge, Cambridge, UK

Electronic Supplementary Information (ESI) available: Experimental methods and supporting figures. See DOI: 10.1039/x0xx00000x

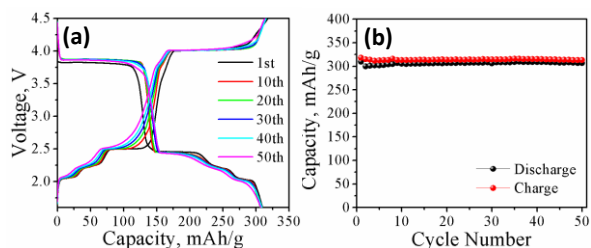


Figure 2. (a) Galvanostatic charge-discharge curves of  $\epsilon$ -VOPO<sub>4</sub> from 1.6 to 4.5 V and (b) cycle performance at C/50, 1C = 2 Li.

This material matches well with our earlier results from Chen et al., where  $\epsilon$ -VOPO<sub>4</sub> synthesized from monoclinic H<sub>2</sub>VOPO<sub>4</sub> are made up of single crystals up to 200 nm.<sup>15</sup> Achieving small primary particles is important for two reasons. First it reduces the Li diffusion length thereby improving the Li<sup>+</sup> intercalation rate. Second, having separated primary particles, rather than agglomerates, allows for an electronically conductive coating to be applied to each particle. This enhances the electron transfer in these electronically insulating materials. Azmi et al. reported that smaller LiVOPO<sub>4</sub> particle size results in easier lithium-ion diffusion with enhanced coulombic efficiency by improving the capacity of lithium deintercalation upon discharge and the decreasing the lithium intercalation potential upon charge.<sup>16</sup> As seen in Figure 1b, pure crystalline  $\epsilon$ -VOPO<sub>4</sub> was produced, resulting in sharp and narrow peaks in the x-ray diffraction pattern. The observed pattern matched very well to the calculated pattern with no impurities or other vanadyl phosphate phases, resulting in a low Rwp value of 4.55%. The cell parameters of the  $\epsilon$ -VOPO<sub>4</sub> are  $a = 7.2670 \text{ \AA}$ ,  $b = 6.8801 \text{ \AA}$ ,  $c = 7.2621 \text{ \AA}$ , and  $\beta = 115.35^\circ$ , very close to the literature values of  $a = 7.2659 \text{ \AA}$ ,  $b = 6.8934 \text{ \AA}$ ,  $c = 7.2651 \text{ \AA}$ , and  $\beta = 115.34^\circ$ .<sup>18</sup> The well-distributed nano-sized  $\epsilon$ -VOPO<sub>4</sub> primary particles provide a good surface area for the carbon additive to wrap around and assist in electron migration during the charge/discharge process, thus, preserving the crystal structure for better reversible intercalation chemistry. Figure 1c and d present TEM images of 75 wt.%  $\epsilon$ -VOPO<sub>4</sub> that was hand milled with 15 wt.% graphene nanoplatelets in a mortar and pestle before adding 10 wt.% PDMF and NMP for electrode preparation. The graphene nanoplatelets form a conductive network that connect the  $\epsilon$ -VOPO<sub>4</sub> primary particles, which increases the electronic and ionic conductivity between these particles. Figure 1d shows that the graphene nanoplatelets coating on the  $\epsilon$ -VOPO<sub>4</sub> particles is around 10 nm.

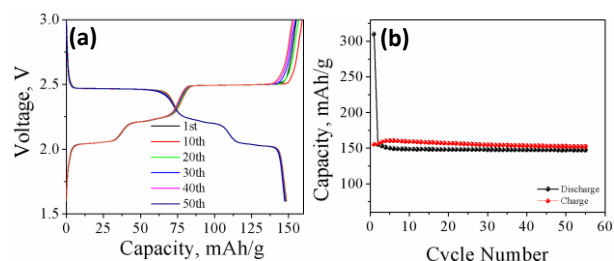


Figure 3. (a) Galvanostatic charge-discharge curves of  $\epsilon$ -VOPO<sub>4</sub> in the low voltage region, from 1.6 to 3.0 V and (b) cycle performance at C/50, 1C = 2Li

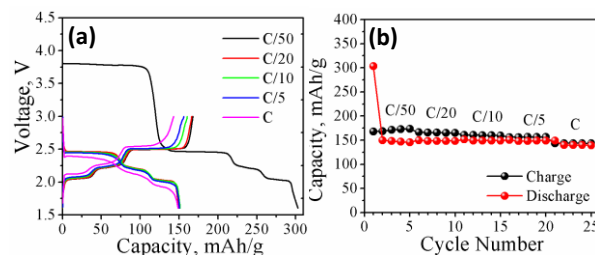


Figure 4. (a) Cycling curves of  $\epsilon$ -VOPO<sub>4</sub> in the low voltage region, from 1.6 to 3.0 V, at different rates and (b) cycle performance

Figure 2a and b shows  $\epsilon$ -VOPO<sub>4</sub> cycling in the whole voltage window from 1.6 V to 4.5 V at C/50, capable of achieving a high discharge capacity of 305 mAh/g for at least 50 cycles. Figure 2a displays the desired characteristic plateaus at  $\sim 4.0$  V at the high voltage region and  $\sim 2.5$ , 2.25, 2.0 V at the low voltage region. The drop from the high voltage region to the low voltage region is a step-like curve and the hysteresis gap between the charge and discharge curve is very small. The high voltage region has a long plateau which extends the capacity to  $\sim 150$  mAh/g, equivalent to  $\sim 1$  Li. This corresponds to the V<sup>5+</sup>/V<sup>4+</sup> redox potential where  $\epsilon$ -VOPO<sub>4</sub> becomes  $\epsilon$ -LiVOPO<sub>4</sub>. The low voltage region has three plateaus at 2.5, 2.25 and 2.0 V which also extends the capacity to  $\sim 150$  mAh/g, corresponding to the second intercalation of lithium where  $\epsilon$ -Li<sub>2</sub>VOPO<sub>4</sub> is formed. The plateaus in the low voltage region have maintained step-like curves even after 35 cycles, showing good kinetics and that the changes in the local structure are reversible. A similar behaviour is observed at the higher C/20 rate (ESI Figure 2).

To determine the reaction rates and reversibility for each redox couple, the intercalation of lithium into  $\epsilon$ -VOPO<sub>4</sub> was also studied separately in the high and low voltage regions. For the V<sup>4+</sup>/V<sup>3+</sup> region study, the  $\epsilon$ -VOPO<sub>4</sub> was first discharged to 1.6 V, and then the cycling was restricted to the V<sup>4+</sup>/V<sup>3+</sup> redox regime, 1.6 V to 3.0 V. In this first discharge, the cell capacity reached 305 mAh/g as expected (Figures 3b and 4b). Figures 3a and b show  $\epsilon$ -VOPO<sub>4</sub> cycled in the low voltage V<sup>4+</sup>/V<sup>3+</sup> region, and a capacity of 150 mAh/g as expected for complete formation of  $\epsilon$ -Li<sub>2</sub>VOPO<sub>4</sub>. The voltage curves clearly show three distinct plateaus at 2.5 V, 2.25 V and 2.0 V. These plateaus agree with DFT calculations confirming the two intermediate phases at  $x = 1.5$  and  $1.75$  in  $\epsilon$ -Li<sub>x</sub>VOPO<sub>4</sub>.<sup>12</sup> Even after 50 cycles, each voltage step is clearly distinguishable, indicating the reversibility of these reactions. No smoothing out of curves was observed,

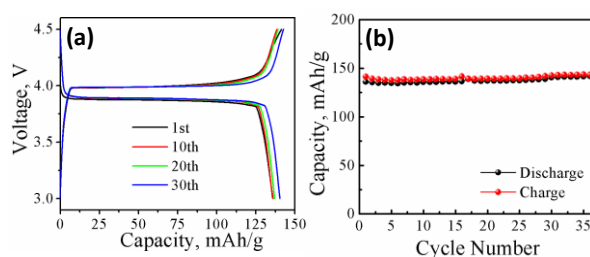


Figure 5. (a) Galvanostatic charge-discharge curves of  $\epsilon$ -VOPO<sub>4</sub> at the high voltage region, from 3.0 to 4.5 V and (b) cycle performance at C/50, 1C = 2Li

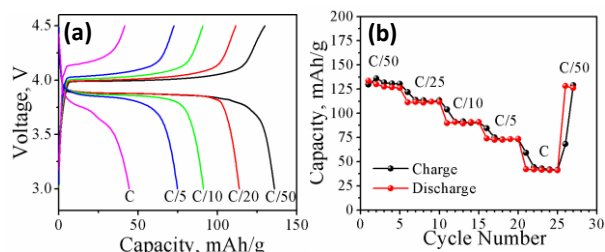


Figure 6. Cycle curves of  $\epsilon$ -VOPO<sub>4</sub> at high voltage region, from 3.0 to 4.5 V, at different current rates and (b) cycle performance

suggesting no structural damage had occurred over these extended intercalation and de-intercalation reactions.

The kinetics of lithium intercalation, for the  $V^{4+}/V^{3+}$  reaction, were determined over a range of C rates. This would also enable us to see if the lithium ordering was retained. The results are shown in Figure 4. As in Figure 3, the cell was first discharged to 1.6 V at the C/50 rate, and then cycled between 1.6 V to 3.0 V. The rate was then increased in steps from C/50 to 1C. The ordering plateaus (Figure 4a) are still distinct even at the highest rates, but at the 1C rate, there is an indication of some smoothing out of the transitions between plateaus. This is an indication of the excellent kinetics of both lithium intercalation and de-intercalation in the compositions from  $\epsilon$ -LiVOPO<sub>4</sub> to  $\epsilon$ -Li<sub>2</sub>VOPO<sub>4</sub>. Consistent with this result, the discharge capacity hardly changes as the rate of reaction changes from C/50 to C, as indicated in Figure 4b. However, the charge capacities increase as the rate of reaction decreases, suggestive of some side-reactions with the electrolyte.

The  $V^{5+}/V^{4+}$  redox couple shows a quite different behaviour to the  $V^{4+}/V^{3+}$  redox couple. As Figure 5a shows, there is a single 3.8 V plateau upon discharge, indicative of a two-phase reaction of  $\epsilon$ -VOPO<sub>4</sub> and  $\epsilon$ -LiVOPO<sub>4</sub> with no intermediate lithium ion ordering. This is consistent with prior reports.<sup>10</sup> The capacity in this material is 140 mAh/g and is approaching the theoretical value of 150 mAh/g. This contrasts earlier literature reports,<sup>11,12</sup> where the capacities were typically less than 100 mAh/g. Figure 5b shows the extended stability of the capacity, which in fact increases slightly on repeated cycling, closer to the theoretical value of 150 mAh/g. This could be related to breaking up of some of the particles allowing more ready access by the electrolyte. This behaviour was earlier seen by Bianchini et al,<sup>13</sup> but in their case the initial capacity was only 80 mAh/g and increased to 135 mAh/g after 30 cycles. The capacity retention seen here is, again, an indication of the stability of the  $\epsilon$ -VOPO<sub>4</sub> lattice to lithium intercalation and de-intercalation. In addition, as shown in Figure 5b, the discharge and charge capacities almost lie on top of another indicative of a coulombic efficiency close to 100%, thus, the absence of side-reactions.

The rate capability of the  $V^{5+}/V^{4+}$  redox couple also shows a different behaviour to the  $V^{4+}/V^{3+}$  redox couple. As can be seen from Figure 6, the capacity falls off rapidly as the rate of the reaction increases. This is indicative of a lower reaction kinetics for this two-phase reaction than for the lithium content beyond 1. However, this is not a result of any damage or change to the crystalline lattice of the VOPO<sub>4</sub>, as the capacity returns to its

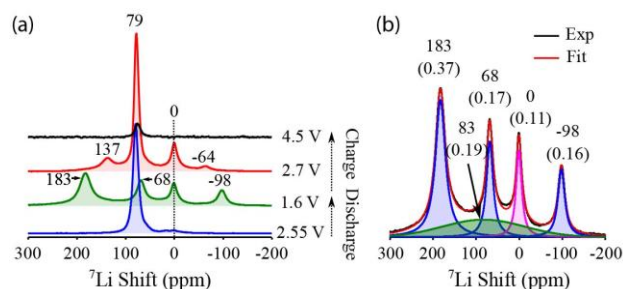


Figure 7 a) Isotropic regions of <sup>7</sup>Li NMR spectra of  $\epsilon$ -Li<sub>x</sub>VOPO<sub>4</sub> materials cycled to different voltages on first charge and subsequent discharge. Spectra were acquired at a magic angle spinning frequency of 60 kHz with an external field of 4.7 T. All spectra are scaled by the sample mass and number of scans. b) Deconvolution (red) of experimental <sup>7</sup>Li spectrum (black) of sample discharged to 1.6 V. The un-bracketed values above the peaks indicate the <sup>7</sup>Li shift in ppm, and the bracketed values indicate the fraction of the total intensity.

original value when the rate is reduced back to C/50. Thus, the structure is preserved.

The ability to reversibly insert two Li in the  $\epsilon$ -VOPO<sub>4</sub> structure was confirmed by <sup>7</sup>Li NMR. Samples of  $\epsilon$ -Li<sub>x</sub>VOPO<sub>4</sub> were cycled to voltages of 2.55 and 1.6 V on first discharge, and 2.7 and 4.5 V on first charge after the first discharge to 1.6 V, at a rate of C/50. The cells were then disassembled for ex-situ NMR analysis and the resulting NMR spectra are shown in Figure 7a. On first discharge to 2.5 V, corresponding to a Li composition of  $x = 1$ , the <sup>7</sup>Li NMR spectrum contains one predominant peak at 79 ppm, which is consistent with Li in  $\epsilon$ -LiVOPO<sub>4</sub>.<sup>19</sup> The dominant mechanism leading to the large Li shifts is due to the Fermi contact interaction with the unpaired electrons on the neighbouring paramagnetic  $V^{4+}$  ( $t_{2g}^1e_g^*0$ ) ions. A small (~1% of total intensity), paramagnetically shifted peak is also present at 18 ppm (ESI Figure 5), which may be due Li in surface sites on the  $\epsilon$ -LiVOPO<sub>4</sub> structure, or local defects within the  $\epsilon$ -LiVOPO<sub>4</sub> bulk, as are seen in similar phosphate materials.<sup>20</sup> A sharp, diamagnetically shifted environment is also present at 0 ppm, which is likely to be due to a small amount of surface impurity, such as Li<sub>2</sub>CO<sub>3</sub> formed during cycling.

On further discharge to 1.6 V, the spectrum contains three paramagnetically shifted Lorentzian type peaks at 183, 68 and -98 ppm, in a ratio of approximately 2:1:1 (Figure 7b). To confirm that the Li environments formed electrochemically were due to the  $\epsilon$ -Li<sub>2</sub>VOPO<sub>4</sub> phase, the <sup>7</sup>Li NMR spectrum of chemically lithiated to  $\epsilon$ -Li<sub>2</sub>VOPO<sub>4</sub> was also acquired (ESI Figure 6). The three paramagnetically shifted peaks in the electrochemically lithiated phase are in good agreement with the chemically lithiated material. They are also consistent with the previous <sup>6</sup>Li NMR study of  $\epsilon$ -Li<sub>2</sub>VOPO<sub>4</sub> by Davis et al,<sup>21</sup> suggesting that Li composition of  $x = 2$  has been successfully reached. The peak at 0 ppm, seen in both the electrochemically lithiated and chemically lithiated samples, has also been observed by Davis et al. They found that it does not exchange with the other sites suggesting that it originates from a different phase.<sup>21</sup> A broad Gaussian peak, centred at 83 ppm, was also required to accurately fit the spectrum in Figure 7b. The broad component suggests that there is some local Li disorder in the  $\epsilon$ -Li<sub>2</sub>VOPO<sub>4</sub> structure. Full details of the deconvolution can be found in the

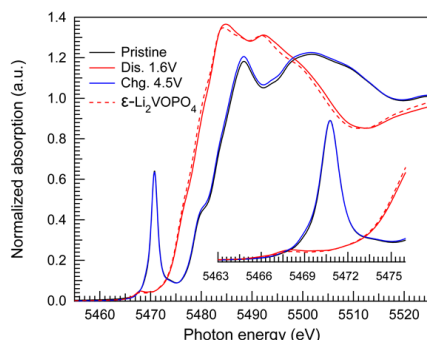


Figure 8. Normalized absorption spectra at the V K-edge of electrochemically discharge/charged samples of  $\epsilon$ -VOPO<sub>4</sub>. The inset shows an enlarged pre-edge region of these spectra

ESI Figure 7. An additional, more intense, diamagnetic environment is also present at 0 ppm in the spectrum at 1.6 V, which may be related to Li containing phases as part of the solid-electrolyte-interface formed at lower voltages.

On discharge to 1.6 V and subsequent charge to 2.7 V, the peak at 79 ppm corresponding to  $\epsilon$ -LiVOPO<sub>4</sub> reemerges as the main resonance. Additional paramagnetically shifted resonances at 137 and -64 ppm are also present. These peaks are tentatively assigned to Li sites in the intermediate  $\epsilon$ -Li<sub>1.5</sub>VOPO<sub>4</sub> structure containing V<sup>3+</sup> ( $t_{2g}^2e_g^*$ ) and V<sup>4+</sup> ( $t_{2g}^1e_g^*$ ) ions. These Li environments may correspond to similar local environments to the sites at 183 and -98 ppm in the  $\epsilon$ -Li<sub>2</sub>VOPO<sub>4</sub> structure, in which all of the vanadium adopt the V<sup>3+</sup> oxidation state. The nature of local environments in  $\epsilon$ -Li<sub>2</sub>VOPO<sub>4</sub> and the intermediate structures,  $\epsilon$ -Li<sub>1.5</sub>VOPO<sub>4</sub> and  $\epsilon$ -Li<sub>1.75</sub>VOPO<sub>4</sub>, will be the subject of future work. On full discharge to 1.6 V and subsequent charge to 4.5 V, only a very weak Li resonance is observed at 79 ppm, indicating that almost all of the Li has been removed from the structure, as  $\epsilon$ -VOPO<sub>4</sub> is silent in the 7Li NMR spectrum. The diamagnetic peak at 0 ppm associated with Li containing phases on the surface of the particles has also been removed on charge.

Ex-situ XAS experiments were also conducted on  $\epsilon$ -Li<sub>x</sub>VOPO<sub>4</sub> electrodes to further confirm the full reversibility of multi-electron V<sup>3+</sup>/V<sup>5+</sup> redox processes in  $\epsilon$ -VOPO<sub>4</sub>. The XAS spectra, as shown in Figure 8, are of electrodes that were discharged to 1.6 V and charged to 4.5 V, both cycled at C/50. For the sample discharged to 1.6 V, there is a shift in the position of the main edge towards lower energy and a decrease in the intensity of the pre-edge peak. Both of these features are similar to those of the  $\epsilon$ -Li<sub>2</sub>VOPO<sub>4</sub> reference compound. These results confirm the reduction of V<sup>5+</sup> to V<sup>3+</sup> upon electrochemical insertion of 2 Li<sup>+</sup> during discharge to 1.6 V. For the sample charged to 4.5 V, both the position of the main edge and the intensity of the pre-edge peak revert to those of the pristine material, indicating concurrent oxidation of V<sup>3+</sup> to V<sup>5+</sup> upon extraction of 2 Li<sup>+</sup> during charge to 4.5 V. Further XAS analysis of cycled  $\epsilon$ -VOPO<sub>4</sub> at different states of charge between 1.6 V and 4.5 V is currently underway.

In conclusion, we show that by controlling the morphology and size of  $\epsilon$ -VOPO<sub>4</sub>, the full electrochemical capacity of the  $\epsilon$ -VOPO<sub>4</sub>/ $\epsilon$ -Li<sub>2</sub>VOPO<sub>4</sub> reaction can be obtained. This reaction is

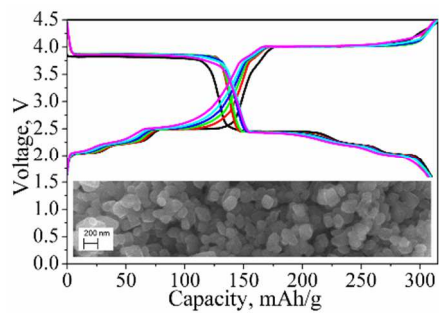
demonstrated to be fully reversible with no observable damage to the material. The kinetics of the intercalation of the first lithium ion is much lower than that of the second lithium ion, where no rate limitations were observed up to the 1C rate.

## Conflicts of interest

There are no conflicts to declare.

## References

- M. S. Whittingham, *Chem. Rev.*, 2004, **104**, 4271–4301
- M. Winter, R. J. Brodd, *Chem. Rev.*, 2004, **104**, 4245–4270
- B. C. Melot, J. M. Tarascon, *Acc. Chem. Res.*, 2013, **46**, 1226–1238
- M. S. Whittingham, *Chem. Rev.* 2014, **114**, 11414–11443
- K. Zaghib, A. Mauger, F. Gendron, C. M. Julien, *Chem. Mater.*, 2008, **20**, 462–469
- H. Liu, F. C. Strohbridge, O. J. Borkiewicz, K. M. Wiaderek, K. W. Chapman, P. J. Chupas, C. P. Grey, *Science*, 2014, **344**, 1252817
- G. Hautier, A. Jain, S. P. Ong, B. Kang, C. Moore, R. Oe, G. Ceder, *Chem. Mater.* 2011, **23**, 3495–3508
- en, Q. Wang, Y. C. Lin, N. A. Chernova, K. Kharki, Y. Chung, F. Omenya, S. Sallis, L. F. J. Piper, S. P. Ong, M. S. Whittingham, *Chem. Mater.*, 2016, **9**, 3159–3170
- S. C. Lim, J. T. Vaughey, W. T. A. Harrison, L. L. Dussack, A. J. Jacobson, J. W. Johnson, *Solid State Ionics* 1996, **84**, 219–226.
- T. A. Kerr, J. Gaubischer, L. F. Nazar, *Electrochem. Solid-State Lett.* 2000, **3**, 460
- Song, Y.; Zavalij, P. Y.; Whittingham, M. S. *J. Electrochem. Soc.* 2005, **152**, A721
- Y. C. Lin, B. Wen, K. M. Wiaderek, S. Sallis, H. Liu, S. H. Lapidus, O. J. Borkiewicz, N. F. Quackenbush, N. A. Chernova, K. Karki, F. Omenya, P. J. Chupas, L. F. J. Piper, M. S. Whittingham, K. W. Chapman, and S. P. Ong, *Chem. Mater.*, 2016, **28**, 1794–1805
- M. Bianchini, J. M. Ateba-Mba, P. Dagault, E. Bogdan, D. Carlier, E. Suard, C. Masquelier, L. Croguennec, *J. Mater. Chem. A*, 2014, **2**, 10182–10192
- O. Xiuqin, P. Lin, G. Haichen, W. Yichen, L. Jianwei, *J. Mater. Chem.* 2012, **22**, 9064
- Z. Chen, Q. Chen, L. Chen, R. Zhang, H. Zhou, N. A. Chernova, M. S. Whittingham, *J. Electrochem. Soc.* 2013, **160**, A1777–A1780.
- B. M. Azmi, H. S. Munirah, T. Ishihara, *Ionics*, 2005, **11**
- K. L. Harrison, C. A. Bridges, C. U. Segre, C. D. Varnado Jr., D. Applestone, C. W. Bielawski, M. P. Paranthaman, A. Manthiram, *Chem. Mater.*, 2014, **26**, 3849–3861
- F. Girgsdies, M. Schneider, A. Brueckner, T. Ressler, R. Schloegl, *Solid State Sci.* 2009, **11**, 1258
- J. M. Ateba-Mba, PhD Thesis, New Transition Metal Fluorophosphates as Positive Electrode Materials for Li-ion Batteries, Univ. Bordeaux, 2013
- R. J. Messinger, M. Ménétrier, E. Salager, A. Boulineau, M. Duttine, D. Carlier, J. M. Ateba-Mba, L. Croguennec, C. Masquelier, D. Massiot, M. Deschamps, *Chem. Mater.* 2015, **27**, 5212–5221
- L. J. M. Davis, X. J. He, A. D. Bain, G. R. Goward, *Solid State Nucl. Magn. Reson.*, 2012, **42**, 26–32



Synthesizing highly crystalline nano-sized  $\epsilon$ -VOPO<sub>4</sub> particles is the key to achieve theoretical capacity of 2 Li<sup>+</sup> intercalation in lithium-ion batteries.